Lifetime Optimization Using Energy Allocation in Wireless Ad-hoc Networks

Davood Shamsi and Farinaz Koushanfar

***Abstract*—We develop energy-balancing strategies for wireless ad-hoc networks energy resource allocation and deployment. The objective is to extend the network lifetime. We find the amount of energy storage that each node requires for having a balanced energy consumption throughout the network. For a limited set of energy resources in the deployment area, we determine an efficient deployment scenario in which messages are routed across the network while using the fastest delivery path. Two ad-hoc architectures are considered: first, where the network is *peer-to-peer* and all the nodes have the same characteristics; and second, a *base-station* centric network where a base-station in the center collects the data from the ad-hoc nodes. We study *synchronous* and *asynchronous* communication paradigms for both architectures.**

To address the problems, we first determine the deployment scheme that results in the most comprehensive radio coverage. Next, we calculate the energy distribution for each network scenario. Then, the derived distributions are extended to randomly deployed networks. We present a thorough analysis and comparison for peer-to-peer and base-station architectures, for both synchronous and asynchronous paradigms. Our experimental evaluations show that the energy-balancing distributions extend the network's lifetime by more than 40% when compared to non-balanced networks with no overhead on message routing delay.

I. INTRODUCTION

Energy is the most scarce resource and constraint in wireless ad-hoc networks (WANs). WANs are often deployed for monitoring and surveillance tasks or to transfer data over a geographic extent. A prime example of their usage is in sensor networks, where sensor-based ad-hoc nodes collect the sensed data from various parts of the environment and then either make autonomous distributed decisions, or collect the distributed data from ad-hoc nodes at a base-station and later fuse the data together to make a decision.

Our objective is to *maximize the duration of the network's lifetime*, without the need for manual interactions and battery replacement. We define lifetime as the time when the first node in the WAN fully depletes its battery [1]–[3]. Note that, disconnecting one node might not disconnect the whole network. However, many experiments reveal that there is a sharp transition point for the WAN disconnection, as many nodes in similar conditions in the network would deplete their energy at once and the non-depleted nodes would be wasted once the network disconnects [4]. Thus, to maximize the efficiency of network's energy consumption, one must *balance* the energy usage of the distributed nodes to prevent the network disconnection. An important observation is that under the assumption that the nodes in the network have a uniform probability of being a transmitter or receiver, the nodes that are deployed in the inner parts of the WAN have a larger probability of being utilized as forwarding relays. For example in Figure 2, node v_n is more likely to be used as a relay node than node v_m.

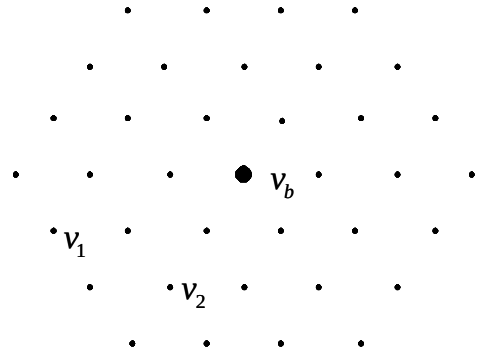

Fig. 1. Base station in the center of area.

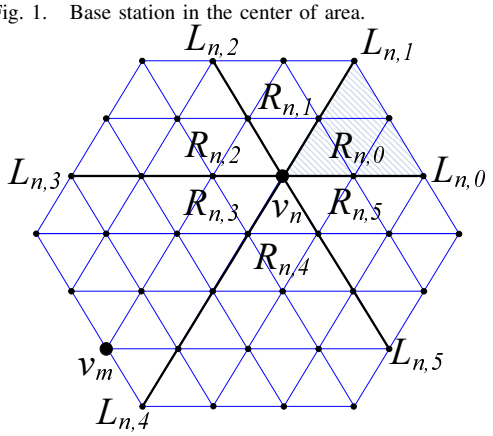

Fig. 2. The triangular grid deployment.

Given a fixed number of nodes' energy sources (batteries), we address the problem of assigning the batteries to the nodes in the deployment field. We find the assignment that balances the energy depletion of the nodes, while the WAN covers the largest possible area and the packets traversing the network are routed on the shortest possible paths with the minimal delay. We consider the *peer-to-peer* and *base-station* architectures, for both *synchronous* and *asynchronous* communication paradigms. In the peer-to-peer architecture, all nodes directly communicate with each other. In base-station architecture, all nodes send their sensed data to a base station v_b in the center of the area. An example is shown in Figure 1. For all cases, we probabilistic analysis for finding the continuous distributions of the energy resource assignment in the area.

Our contributions are as follows. First, we find the energy-balancing distribution of the nodes energy resources by using analytical methods. Second, the distributions take into

account the effect of the important component of the *idle energy* consumption. To the best of our knowledge, this component has not been considered in any of the previous work that addressed relevant energy distribution problems [5]–[7]. Third, we present a detailed comparison between the energy-balancing distributions of peer-to-peer and base-station architectures in terms of lifetime, coverage area, and delay overhead for the equal amount of available energy resources. Fourth, we carefully examine and compare the energy balancing distributions and their properties in synchronous versus asynchronous communication paradigms. Fifth, scaling and asymptotic properties of the derived distributions both in terms of the number of nodes and the amount of available energy resource are explored. Sixth, we show that the derived distributions can be used for randomly deployed networks by evaluating their energy-balancing properties. Proposed distributions cause more efficient randomly deployed network. Lastly, we show how balanced distributions can be applied to the large networks with multiple base-stations.

The remainder of the article is organized as follows. After describing the preliminaries in the next section, we survey the related literature in Section II. Section IV presents the problem statements. The analytical solution to the problems are presented in Section V. We extend the derived energy distributions to the random networks and the networks with multiple base stations in Subsection V-E2. The evaluations and comparisons of various scenarios are discussed in Section VI. We conclude in Section VII.

II. RELATED WORK

System level power management of wireless ad-hoc networks has recently attracted a lot of attention [8]–[15]. Generally, lifetime maximization methods can be divided in two main categories: pre-deployment lifetime maximization methods [10], [16]–[19] and post-deployment lifetime maximization methods [20] [21] [22] [23]. In the former, node's positions (or distribution or energy level) are determined to maximize networks' lifetime. The later methods try to maximize the networks' lifetime when nodes are already deployed and there is no control on node positions. The work that is presented in this paper focuses on the pre-deployment lifetime maximization.

A number of research groups have derived upper bounds for the lifetime of a multi-hop WANs or wireless sensor networks [5], [7]. These upper bound are derived for networks that collect information form a specific area and send it to a base-station. Also, heuristic methods for placement of the nodes for minimizing the energy consumption were proposed [24], [25]. Subramanian and Fekri [26] propose a non-uniform distribution of nodes in the area for a data gathering scenario with a base-station, where all the nodes are actively sending data in each time interval.

In sensor networks, several schemes for distribution of sensor energies over a sensing field where the quality of the reconstructed sensed phenomena additionally constraints the placement of sensors have been addressed [10], [16]–[18]. For example, Iranli et al. have developed deployment strategies for a two-tier wireless sensor networks for monitoring the sensed phenomena [10]. The two-tier is composed of nodes (sensors) and microservers (data gathering and forwarding units). The authors have solved the problem of assigning energy to components such that the network lifetime is maximized subject to a total energy budget. In another work, Maleki and Pedram [18] found the sensor node density, at every point inside a given deployment region which results in allocating the minimum total number of sensors.

Another pre-deployment lifetime maximization method is introduced by Krause *et al.* [19], where nodes collect data and send it to a base-station. Node placement over the information field is their main concern. They have introduced a placement algorithm to maximize information gathered by network while minimizing the network energy consumption. They have modeled the information field and inter-node link qualities by Gaussian processes. Then, based on the models, communication cost and sensing quality are predicted. Finally, using the predictions, they propose a heuristic algorithm for node placement. It is assumed that all nodes can communicate directly, *i.e.*, no multi-hop communication is assumed. Moreover, they do not consider idle the energy consumption and assume that the network is fully synchronized.

The work presented herein adds to the knowledge of the existing literature in a number of ways. First, our work considers the idle energy consumption in the distribution derivations. Second, it also addresses the problem for both synchronous and asynchronous cases. There are a number of heuristic placement methods [24], [25] that consider the idle energy but do not derive any analytical distributions or bounds. None of the analytical schemes consider the effects of the idle energy or asynchrony in deriving the distribution function or the upper bounds [5]–[7], [10], [16]–[19], [24]–[26]. Third, the comparisons between the peer-to-peer and base-station networks for synchronous and asynchronous cases were not performed before. Lastly, we show how the analytically derived distributions can be applied to randomly deployed networks and large networks with multiple base stations. Note that we do not address sensing: the distribution of the sensed phenomena that has a great impact on the analytical distribution derivations varies across environments. Unless a specific phenomenon and a model (or a learning method) is assumed, it is hard to generalize the sensed phenomena. We express that deriving the balanced nodes distributions for communicating messages would pave the way for the analysis of sensor data, assuming known or learnable models of the physical entity [19], [27].

III. PRELIMINARIES

In this section, we describe preliminaries, including the definitions and our assumptions.

• *Energy consumption model.* Several studies of node's energy consumption have revealed that the radios are the most significant sink of the node's limited battery energy. Radios do not just consume energy while sending and receiving packets, but also they consume a non-negligible amount of energy when they are listening (idle) [28]. Table I shows the energy consumption for different technologies.

• *Energy balancing.* Assignment of energy resources to nodes such that the nodes deplete their energies in the same time is called energy balancing. In our analysis and simulations, we divide operation time of the network into intervals of time with the same length, denoted by *time step*.

• Nodes wake up for a short interval at each time step.

TABLE I
ENERGY CONSUMPTION IN DIFFERENT TECHNOLOGIES

Technology	Receive (mW)	Transmit (mW)	idle (mW)
MICA2 Mote [29]	30	81	30
LUCENT IEEE 802.11 Wavelan PC card (2 Mbps) [28]	960	1330	843
Orinoco Gold 802.11b PCMCIA [30]	3500	3700	2380

• *Lifetime.* Number of time steps during which all the nodes are alive.

• *Nodes' radio coverage.* The unit disk radio model is assumed: two nodes that are closer than a given radio range r can directly communicate. The further nodes use the nodes within their radio range to relay (forward) the messages in a multi-hop way. A node's radio has many power levels that translate to different received signal powers or *achievable radio ranges* (i.e., the longest distance in which the packets are received with a very high probability). To optimize the coverage, we consider the ratio of the achievable radio range (R) to the transmission power consumption (P_t) of the nodes $\frac{R}{P_t}$ that has a maximal point for the radio in a certain homogeneous environment. In the most reported range studies the maximum is achieved by setting the radio at its highest level. We use the maximum $\frac{R}{P_t}$ as the operational point of the transmission for all nodes that provides the largest and the most energy-efficient coverage area. Note that it is proved deployment in Figure 2 provides the maximum coverage area [31].

• *Synchronization.* Two nodes are synchronized if and only if their clocks present exactly the same time. We study both synchronous and asynchronous communication paradigms. In synchronous, at each time step, there is a small interval of time where the nodes all wake up together and poll their neighbors to check for new messages. The nodes save their energy by sleeping the remainder of the time step. In asynchronous network, nodes sleep in durations to save power as well. But the nodes that are sending or forwarding have to wait for the asleep neighbor to wake up before relaying for them. Thus, the waiting nodes waste energy while they are idle [32].

• *Deployment.* To maximize the coverage, nodes are deployed in a triangular grid deployment that provably provides the maximal coverage for the unit disk model [31] when not considering energy balancing. The distance between the nodes is determined by the maximum $\frac{R}{P_t}$ of the environment. A small triangular deployment grid is illustrated in Figure 2. Nodes are regularly placed in the vertices of triangles. Length of edges in triangles are equal to communication range of nodes. We consider a symmetric deployment area and perform our analysis on this network. However, as we show in our evaluations, the distributions resulting from our analysis provide a bound for the achievable coverage and provide energy balancing even for the random deployment scenarios.

• *Network Architecture.* We study (i) a peer-to-peer architecture, where all the nodes equivalent capacities; and (ii) a base-station centric architecture, where all messages are sent to and received from the base-station. The base-station is located in the center of the monitoring area (Figure 1).

• *Routing.* The routing strategy is assumed to be the shortest path. Note that one could potentially design a routing strategy for balancing the energy consumption of the nodes. However, assuming a lossless channel, a longer route means a larger delay and more energy consumption that is not desirable. The proposed energy balancing method guarantees the shortest path routing time while optimizing for a balanced energy distribution.

IV. PROBLEM FORMULATION AND ASSUMPTIONS

In this subsection, we present the formal definition of our problem and the four considered scenarios. If the goal is to simultaneously address the coverage and energy efficiency, the problem is NP-complete and computationally intractable [33]. We decided to fix the deployment to a symmetric grid coverage shape and study the distributions. Note that in Subsection V-E2, we explain how the derived distributions (for the symmetric regular deployment) can be extended to the randomly deployed networks.

PROBLEM: Balancing of Energy in Deployment of WANs (BalancED).

Instance: An ad-hoc network with N nodes, $\{v_1,\ldots,v_N\}$, each with a maximum radio range r, in a symmetric deployment field *F* (the topology was described in Section III), where all the nodes have identical probabilities of being the initial sender or the final receiver of a packet.

Question: Find the distribution of the nodes' energies such that all the nodes deplete their energy the same time and the network arrangement does not increase the path delays, i.e., shortest path routes are always used.

Assumptions and comments:

(1) We assume the shortest path routing. When there are more than one shortest path between the sender and the receiver, we use the following policy to route the packets. When node v_n wants to send a packet to node v_m, it asks its neighbors for the shortest path to the v_m. If there is just one neighbor with the shortest path to v_m then v_n sends the packet to the neighbor with the shortest path. If there are more than one neighbor with the shortest path to v_m, node v_n selects one of them randomly (equiprobably) and sends the pack to the selected neighbor. This procedure is continued until the packet reaches its destination. In this routing policy, each node should just store the local information about the shortest path.

(2) We divide the the network lifetime to a number of time steps. In each time step, one node v_s sends a packet to another node v_r. If there are q hops between v_s and v_r then the packet would be forwarded q times in one time step. Since in each time step, just one packet is delivered, there is *no contention* in the network.

(3) Energy balancing increase the lifetime of the network. Assume the network is not balanced and the total amount of

energy is constant. When energy of the first node is depleted, we say the network is dead. Since the network is not balanced, other nodes still have energy but we consider the network as a dead network. Let assume node v_n is the first node that dies and v_m still has energy. If one increase the energy level of node v_n by decreasing energy level of ode v_m (energy balancing), node v_m would die later. Thus, lifetime of the network is increased.

(4) Although we solve energy balancing problem for symmetric deployment, in Section V-E2, we extend the results to the randomly deployed networks and we do not assume nodes with different amount of energy.

The four considered scenarios are as follows.

(i) BalancED-P2P-s. We address the BalancED-P2P-s problem assuming that all nodes are equivalent, inter-node communication is *peer-to-peer*, and the nodes are all *synchronized*. *i.e.*, a randomly selected node sends a packet to another randomly selected node at a synchronized time step.

(ii) BalancED-P2P-a. We address the BalancED-P2P-a problem assuming that all nodes are equivalence, communication is *peer-to-peer* and nodes are *not synchronized*.

(iii) BalancED-Base-s. We address the BalancED-Base-s problem assuming a *base station* with no power constraint in the middle and nodes are all *synchronized*.

(iv) BalancED-Base-a. We address the BalancED-Base-a problem assuming a *base station* with no power constraint in the middle and nodes are *not synchronized* .

V. Energy-Balancing

The objective of this section is to find the distributions of the consumed energy for different scenarios. To balance the energy usage, we assign the node batteries according to the analytically derived energy consumption. Equivalently, nodes with equal energy can be distributed according to the derived distributions.

A. BalancED-P2P-s

We assume that in a fully synchronized network, nodes periodically and simultaneously wake up for a short time interval to check for packets. There is a fixed energy cost (E_{moni}) for the periodic monitoring. There are three possible states for a communicating node: (1) the node is the initial sender, (2) it is the final receiver, or (3) it is the relay node (forward). For a node v_n, the probabilities of the three states are denoted by (1) $p_s(v_n)$, (2) $p_r(v_n)$, and (3) $p_f(v_n)$. The required energy for the states are denoted by (1) E_s (sending energy), (2) E_r (receiving energy), and (3) E_f (receiving and forwarding energy) respectively. The total communication energy consumption of v_n at one time step is denoted by $E_{step}(v_n)$ that is

$$E_{step}(v_n) = p_s(v_n)E_s + p_r(v_n)E_r + p_f(v_n)E_f \qquad (1)$$

Since E_{moni} is a fixed overhead for all nodes we omit it in derivations.

We now compute the probability terms in Equation 1. Assume that at each time step, a node is randomly selected to send a message to a randomly selected destination node. The assumption of one node at a time is only to clarify the analysis. Extension to multiple nodes could be easily accomplished by scaling in time.

Since all nodes can be equiprobably senders or receivers, for a network of N nodes, $p_s(v_n)$=$p_r(v_n)$=$\frac{1}{N}$. For determining the forwarding probability, we utilize the network topology illustrated on Figure 2, where a randomly selected node v_n is the center of the star formed by the triangle laterals around it. As can be seen on the figure, we define two subsets of nodes as follows

$$\begin{aligned} R_{n,i} &= \{\text{Nodes } \textit{in} \text{ the region } R_i\} \qquad i = 0, \ldots, 5 \\ L_{n,i} &= \{\text{Nodes } \textit{on} \text{ the line } L_i\} \qquad i = 0, \ldots, 5 \end{aligned} \qquad (2)$$

The forwarding probability (p_f) can be found by

$$p_f(v_n) = \sum_{i=0}^{5} p_f(v_n \mid \mathcal{A}_{n,i})\, p_f(\mathcal{A}_{n,i}) + \qquad (3)$$

$$+ \sum_{i=0}^{5} p_f(v_n \mid \mathcal{B}_{n,i})\, p_f(\mathcal{B}_{n,i}) \qquad (4)$$

$$+ \sum_{i=0}^{5} p_f(v_n \mid \mathcal{C}_{n,i})\, p_f(\mathcal{C}_{n,i})$$

$$+ \sum_{i=0}^{5} p_f(v_n \mid \mathcal{D}_{n,i})\, p_f(\mathcal{D}_{n,i})$$

$$+ \sum_{i=0}^{5} p_f(v_n \mid \mathcal{F}_{n,i})\, p_f(\mathcal{F}_{n,i})$$

where $\mathcal{A}_{n,i} = \{R_{n,i} \rightarrow R_{n,i+3(\text{mod } 6)}\}$; $\mathcal{B}_{n,i} = \{L_{n,i} \rightarrow G_{n,i}\}$; $G_{n,i} = L_{n,i+2(\text{mod } 6)} \cup R_{n,i+2(\text{mod } 6)} \cup R_{n,i+3(\text{mod } 6)} \cup L_{n,i+4(\text{mod } 6)}$; $\mathcal{C}_{n,i} = \{L_{n,i} \rightarrow L_{n,i+3(\text{mod } 6)}\}$; $\mathcal{D}_{n,i} = \{R_{n,i} \rightarrow L_{n,i+3(\text{mod } 6)}\}$; and $\mathcal{F}_{n,i} = \{R_{n,i} \rightarrow L_{n,i+4(\text{mod } 6)}\}$. Note that $A \rightarrow B$ means that a node in A sends a packet to a node in B. The "(mod 6)" terms appear because of the hexagonal shape of area, *i.e.*, since indices are ordered, $i + k(\text{mod } 6)$ means k indices away from i.

Deriving elements of Equation 3

To find $p_f(v_n)$, one needs to calculate all the elements in Equation 3. We begin with finding the probability $p_f(A \rightarrow B)$ when A and B are two disjoint sets. Let $v_a \in A$ and $v_b \in B$; thus, $p_f(v_a \rightarrow v_b) = \frac{1}{N(N-1)}$. Also, if $v_a \neq v_c$ then $\{v_a \rightarrow v_b\}$ and $\{v_c \rightarrow v_d\}$ are disjoint. Therefore,

$$\begin{aligned} p_f(A \rightarrow B) &= \sum_{v_a \in A, v_b \in B} p_f(v_a \rightarrow v_b) \\ &= \sum_{v_a \in A, v_b \in B} \frac{1}{N(N-1)} = \frac{\mid A \mid\mid B \mid}{N(N-1)} \end{aligned} \qquad (5)$$

Using Equation 5, all of the non-conditional terms in the Equation 3 can be found.

Before explaining how $p_f(v_n)$ is derived, recall that it is assumed that routing is the shortest path (Section III): each node forwards the packet to one of its neighbors that has the least number of hops to the destination. In case there are multiple such neighbors, one of them will be randomly selected. As Figure 3 shows, there might be more than one shortest path between two nodes.

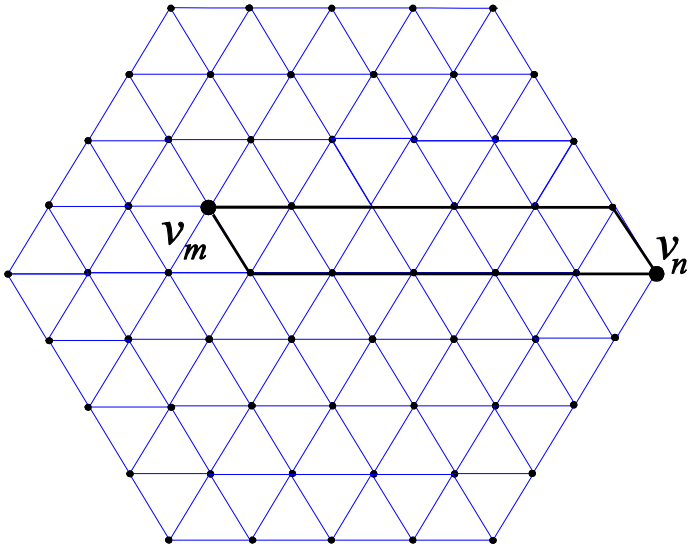

Fig. 3. There might be more than one shortest path between two nodes.

To find the conditional terms of $p_f(v_n)$, we start with those terms that contain $R_{n,i}$ as the transmitter, *i.e.*, $\mathcal{A}_{n,i}, \mathcal{D}_{n,i}, \mathcal{F}_{n,i}$. Suppose that a node v_m in $R_{n,i}$ is sending a packet to the node v_n, as shown in Figure 2. Let $S_{v_m \to v_n,i}$ denote the number of hops traversed along the lines parallel to $L_{n,i}$ in $R_{n,i}$ and $T_{v_m \to v_n,i}$ denote the number of hops traversed along the lines parallel to $L_{n,i+1(\text{mod } 6)}$ in the region $R_{n,i}$.

Consider the case of a node v_m in $R_{n,i}$ is sending a packet to a node in $R_{n,i+3(\text{mod } 6)}$. While the packet is in region $R_{n,i}$ or on its border, it randomly selects one of its two options for the shortest path to the destination. To reach v_n, the packet should do exactly $S_{v_m \to v_n,i}$ movements along line $L_{n,i}$ in its first $S_{v_m \to v_n,i} + T_{v_m \to v_n,i}$ movements. Thus

$$p_f\left(v_n \mid v_m \to R_{n,i+3(\text{mod } 6)}\right) = \frac{\begin{pmatrix} S_{v_m \to v_n,i} + T_{v_m \to v_n,i} \\ S_{v_m \to v_n,i} \end{pmatrix}}{2^{S_{v_m \to v_n,i} + T_{v_m \to v_n,i}}}. \tag{6}$$

Assuming that the sender is in $R_{n,i}$, the probability of the node $v_m \in R_{n,i}$ be the sender is $\frac{1}{|R_{n,i}|}$. Furthermore, if v_a and v_c are two nodes and $v_a \neq v_c$, the probability of the both nodes being senders in the same time is zero. Therefore,

$$p_f\left(v_n \mid R_{n,i} \to R_{n,i+3(\text{mod } 6)}\right) = \frac{1}{\mid R_{n,i} \mid} \sum_{m \in R_{n,i}} \frac{\begin{pmatrix} S_{v_m \to v_n,i} + T_{v_m \to v_n,i} \\ S_{v_m \to v_n,i} \end{pmatrix}}{2^{S_{v_m \to v_n,i} + T_{v_m \to v_n,i}}}. \tag{7}$$

In case that a node v_m in $R_{n,i}$ sends a packet to the a node on the line $L_{n,i+3(\text{mod } 6)}$, if the packet reaches the line $L'_{n,i} = L_{n,i} \cup \{v_n\} \cup L_{n,i+3(\text{mod } 6)}$, it cannot deviate from that line until it reaches the destination. If the packet reaches the line $L'_{n,i}$ exactly after k steps, in the $(k-1)$-th step, it would be adjacent to the line $L'_{n,i}$. Furthermore, at the $(k-1)$-th step, the packet randomly selects between two possible options; moving to line $L'_{n,i}$ or moving parallel to it. Therefore, the packet reaches the line $L'_{n,i}$ exactly after k steps with a probability,

$$\frac{1}{2} \frac{\begin{pmatrix} k-1 \\ T_{v_m \to v_n,i} - 1 \end{pmatrix}}{2^{k-1}}. \tag{8}$$

As can be seen on Figure 2, the packet sent by node v_m passes through the node v_n on its route if it touches line $L'_{n,i}$ in $T_{v_m \to v_n,i}$, $T_{v_m \to v_n,i} + 1$, ..., or $T_{v_m \to v_n,i} + S_{v_m \to v_n,i}$ steps. Therefore,

$$p_f\left(v_n \mid m \to L_{n,i+3(\text{mod } 6)}\right) = \frac{1}{2} \sum_{k=S_{v_m \to v_n,i}}^{T_{v_m \to v_n,i} + T_{v_m \to v_n,i}} \frac{\begin{pmatrix} k-1 \\ S_{v_m \to v_n,i} - 1 \end{pmatrix}}{2^{k-1}}. \tag{9}$$

Such as the previous case, the probability that node v_m be the transmitter provided that it is a member of $R_{n,i}$, is $\frac{1}{|R_{n,i}|}$. Thus

$$p_f\left(v_n \mid R_{n,i} \to L_{n,i+3(\text{mod } 6)}\right) = \frac{1}{2 \mid R_{n,i} \mid} \sum_{v_m \in R_{n,i}} \sum_{k=T_{v_m \to v_n,i}}^{T_{v_m \to v_n,i} + S_{v_m \to v_n,i}} \frac{\begin{pmatrix} k-1 \\ T_{v_m \to v_n,i} - 1 \end{pmatrix}}{2^{k-1}}. \tag{10}$$

Similarly, we find that

$$p_f\left(v_n \mid R_{n,i} \to L_{n,i+4(\text{mod } 6)}\right) = \frac{1}{2 \mid R_{n,i} \mid} \sum_{m \in R_{n,i}} \sum_{k=S_{v_m \to v_n,i}}^{S_{v_m \to v_n,i} + T_{v_m \to v_n,i}} \frac{\begin{pmatrix} k-1 \\ S_{v_m \to v_n,i} - 1 \end{pmatrix}}{2^{k-1}}. \tag{11}$$

Now, we have found the conditional terms in Equation 3, where the transmitter is in $R_{n,i}$. It remains to find the terms that are corresponding to the transmitters being in $L_{n,i}$. Consider the case where node v_m in $L_{n,i}$ sends a packet to a node in $G_{n,i}$. It requires $T_{v_m \to v_n,i}$ movements along $L'_{n,i}$ to reach v_n; in each movement, it is possible to deviate from the line $L'_{n,i}$ with a probability $\frac{1}{2}$. Therefore, the packet visits v_n with a probability $\left(\frac{1}{2}\right)^{T_{v_m \to v_n,i}}$. Knowing that the transmitter is in $G_{n,i}$, the probability of selecting a particular $v_m \in G_{n,i}$ as the transmitter is $\frac{1}{|G_{n,i}|}$. Thus

$$p_f\left(v_n \mid L_{n,i} \to G_{n,i}\right) = \frac{1}{\mid G_{n,i} \mid} \sum_{v_m \in G_{n,i}} \left(\frac{1}{2}\right)^{T_{v_m \to v_n,i}} \tag{12}$$

Finally, we find the probability that a node v_n participates in forwarding when a sender node in $L_{n,i}$ transmits a packet to a receiver node in $L_{n,i+3(\text{mod } 6)}$. In this case, since there is only one shortest path and it includes node v_n, the packet that is sent from a node on $L_{n,i}$ to a node on $L_{n,i+3(\text{mod } 6)}$ passes through node v_n with probability 1, $p_f\left(v_n \mid L_{n,i} \to L_{n,i+3(\text{mod } 6)}\right) = 1$.

In Figure 2, we see that the number of nodes in various subsets $R_{n,i}$ and $L_{n,i}$ are different. Depending on the position of the v_n within the network and its associated subregions, $p_f(v_n), n = 1 \ldots N$ are different. Substituting the derived terms in Equation 1 determines the expected energy consumption for each node.

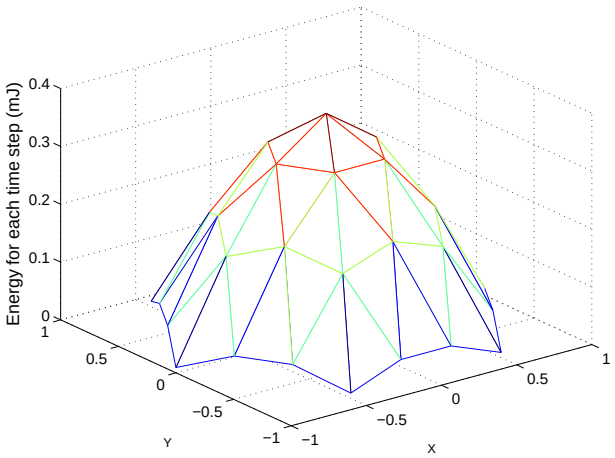

Fig. 4. Energy distribution for asynchronous network. The x and y axes show the deployment coordinates

Figure 4 plots the energy distribution for 61 nodes in a hexagonal area. The x and y axes show the deployment coordinates. The expected energy for each node at one time step is computed by Equation 1, ignoring the fixed monitoring overhead, for $E_{moni} = 0$, $E_s = 1$mJ, $E_r = 1$mJ, and $E_f = 2$mJ.

B. BalancED-P2P-a

In an asynchronous network, nodes are assumed to have periodic cycles of sleeping and waking up for monitoring, similar to the synchronous scenario. However, because of the lack of synchrony among the node's schedules, an awake node (v_n) that receives a packet, cannot immediately forward it to its next neighbor on the shortest path (v_m), until the node's next wake-up. Thus, v_n will consume idle energy.

1) Formulating Energy Distribution as an Optimization Problem: In an asynchronous network, nodes require energy for four tasks: sending a packet, receiving a packet, forwarding a packet, or waiting for the next node in the shortest path to wake up to relay their message. We have already found the required energy for sending, receiving, and forwarding in BalancED-P2P-s. To calculate the idle energy consumption, the sleep duration model for a node v_m is assumed to be a random variable with the expected value α_m. Note that a periodic sleep schedule would be a special case of this model, where the expected value is exactly the sleep duration. Furthermore, the expected value of the sleep duration of each node α_m is assumed to be inversely proportional to the node's initial available energy, i.e., the nodes with larger energy resources wake up more frequently. Thus, they forward more packets. More formally, $\alpha_m = \frac{\lambda_0}{E_t(v_m)}$, where $E_t(v_m)$ is the total energy of node v_m and λ_0 is a constant factor that indicate wake up frequency. If we set up the network such that is can works for J time steps then $E_t(v_m) = JE_{step}(v_m)$. Thus, $\alpha_m = \frac{\lambda}{E_{step}(v_m)}$; where $\lambda = \frac{\lambda_0}{J}$

To find the expected value of the idle energy consumption, assume that node v_n is waiting for its neighbor v_m to wake up and get the packet. The expected wake up time for v_m is α_m seconds (see Appendix D), during which the node v_n consumes idle energy $E_{n_{idle}} = \alpha_m p_w$. p_w is the node's power consumption while it is idle ($E_{n_{idle}}$ is the corresponding energy). Thus, we can find the total node's energy in each time step.

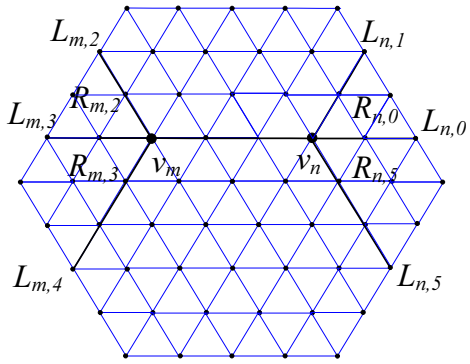

Fig. 5. Node v_n sends a packet to its neighbor v_m. The division of the lines and the regions is also depicted.

$$E_{step}(v_n) = p_s(v_n)E_s + p_r(v_n)E_r + p_f(v_n)E_f + \sum_{v_m \in \mathcal{N}(v_n)} p_{v_n \to v_m} \frac{\lambda p_w}{E_{step}(v_m)} \quad (13)$$

where $p_{v_n \to v_m}$ is the probability that the node v_n sends a packet to its neighbor node v_m and $\mathcal{N}(v_n)$ denotes the nodes that are neighbors of v_n.

The only parameters that we still have not computed in Equation 13 are $p_{v_n \to v_m}$ terms that are derived in Appendix A.

Even though Equation 13 computes the energy that is needed for each node, solving it to the find energy distribution for all nodes in the network might not be not energy efficient. It is so because Equation set 13 does not consider topological aspect of the problem. To clarify, assume node v_m is located on the border of the area. Node v_m is unlike to participate in forwarding and needs less energy than other nodes. Thus, the expected value of its sleep time is large. When v_m is supposed to receive a packet, its neighbor that has the packet, should wait for a long time till node v_m wakes up; hence, it would waste energy. To mitigate this problem, we let nodes have more energy than they need to do their tasks (Equation 13). Then, the total energy in the network will be minimized. We change equalities in Equations 13 to inequalities and call them principal energy inequalities for wireless network. Therefore, we need to find the solution to the following optimization problem.

$$\begin{gathered} \min \quad \sum_{n=1}^{N} E_{step}(v_n) \\ E_{step}(v_n) \geq p_s(v_n) E_s + p_r(v_n) E_r \\ + p_f(v_n) E_f + \sum_{v_{n_i} \in \mathcal{N}_n} p_{v_n \to v_{n_i}} \frac{\lambda'}{E_{step}(v_{n_i})} \quad n = 1 \ldots N \end{gathered} \quad (14)$$

where $\lambda' = p_w \lambda$.

Note that, in Equation 13, we assumed the wake up energy for nodes is zero. One can include wake up energy of the nodes by modifying Equation 13. Based on the wake up policy

discussed in Appendix D, average sleep duration determines wake up frequency. Shorter sleep duration results in higher wake up frequency. i.e, wake up frequency of node $v_n \propto \alpha_n^{-1}$; thus, wake up frequency of node $v_n \propto E_{step}(n)$. Hence, wake up energy adds a linear term in Equation 13.

2) Convex approximation for the optimal solution of energy distribution: Optimization (14) is generally a hard problem. Therefore, we try to approximate it by a convex formulation.

In the first step, consider the following change of variable:

$$U_n = \frac{1}{E_{step}(v_n)}. \tag{15}$$

Thereupon, optimization problem 14 can be restated as

$$\begin{array}{c} \min \quad \sum_{n=1}^{N} \frac{1}{U_n} \\ \left(p_s\left(v_n\right) E_s + p_r\left(v_n\right) E_r + p_f\left(v_n\right) E_f\right) U_n \\ + \sum_{v_{n_i} \in \mathcal{N}_n} p_{v_n \to v_{n_i}} \lambda' U_{n_i} U_n \leq 1 \quad n = 1 \ldots N. \end{array} \tag{16}$$

To formulate Equation (16) in a more compact way, assume H_n is an $N \times N$ matrix where

$$\left(H_n\right)_{i,j} = \begin{cases} p_{v_n \to v_j} \lambda' & i = n, \quad v_j \in \mathcal{N}_n; \\ 0 & \text{otherwise.} \end{cases} \tag{17}$$

$\left(H_n\right)_{i,j}$ denotes the i,j-th element of A. Also, define $\mathbf{U}$ and $\mathbf{b}_n$ be $N \times 1$ matrices where $\left(\mathbf{U}\right)_{n,1} = U_n$, $n = 1 \ldots N$, and

$$\left(\mathbf{b}_n\right)_{i,1} = \begin{cases} p_s\left(v_n\right) E_s + p_r\left(v_n\right) E_r + p_f\left(v_n\right) E_f & i = n; \\ 0 & i \neq n. \end{cases} \tag{18}$$

Hence, we can rewrite Equation 16 as

$$\begin{array}{c} \min \quad \sum_{n=1}^{N} \frac{1}{U_n} \\ \mathbf{b}_n^T \mathbf{U} + \mathbf{U}^T H_n \mathbf{U} \leq 1 \quad n = 1 \ldots N. \end{array} \tag{19}$$

To simplify Equation 19, let

$$\mathcal{U} = \begin{bmatrix} 1 \\ \mathbf{U} \end{bmatrix}, \mathcal{H}_n = \begin{bmatrix} 0 & \frac{1}{2}\mathbf{b}_n^T \\ \frac{1}{2}\mathbf{b}_n & H_n \end{bmatrix}. \tag{20}$$

Thus, we restate Equation 19 as

$$\begin{array}{c} \min \quad \sum_{n=1}^{N} \frac{1}{U_n} \\ \mathcal{U}^T \mathcal{H}_n \mathcal{U} \leq 1 \quad n = 1 \ldots N. \end{array} \tag{21}$$

Now, let $Z = \mathcal{U}\mathcal{U}^T$. Also,

$$\text{trace}\left(\mathcal{H}_n Z\right) = \text{trace}\left(\mathcal{H}_n \mathcal{U}\mathcal{U}^T\right) = \text{trace}\left(\mathcal{U}^T \mathcal{H}_n \mathcal{U}\right) = \mathcal{U}^T \mathcal{H}_n \mathcal{U} \tag{22}$$

Therefore, Equation 21 is equivalent to

$$\begin{array}{c} \min \quad \sum_{n=1}^{N} \frac{1}{U_n} \\ \text{trace}\left(\mathcal{H}_n Z\right) \leq 1 \quad n = 1 \ldots N \\ \text{rank}\left(Z\right) = 1 \\ Z \succeq 0, \end{array} \tag{23}$$

where $Z \succeq 0$ means that Z is semi-positive definite.

Until this point, we have had neither relaxation nor approximation. In other words, we have only restated Equation 16 in a simpler form. To convert it to a convex programming, we apply one approximation and one relaxation. First, we do approximation by changing the objective function from $\sum_{n=1}^{N} \frac{1}{U_n}$ to $-\text{trace}\left(Z\right) = -1 + \sum_{n=1}^{N} -U_n^2$, *i.e.*, instead of minimizing $\sum_{n=1}^{N} \frac{1}{U_n}$, we minimize $-\text{trace}\left(Z\right) = -1 + \sum_{n=1}^{N} -U_n^2$. Moreover, we relax the optimization problem Equation 23 by removing rank-one constrain which is an NP-hard constrain [34]. By these changes, Equation 23 is lifted to the following semi-definite programming (SDP).

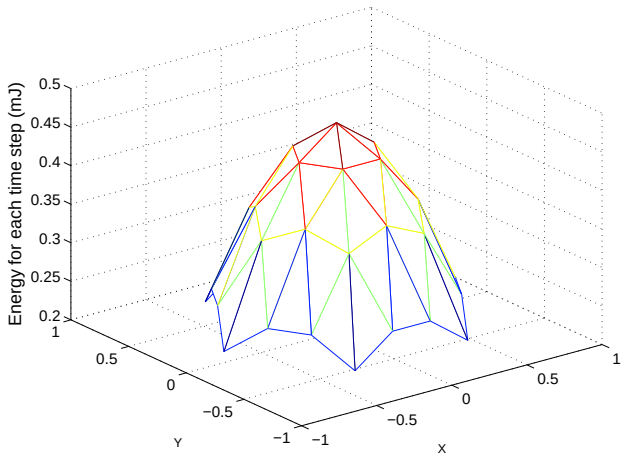

Fig. 6. Energy distribution for asynchronous network. The x and y axes illustrate the deployment coordinates.

$$\begin{array}{c} \min \quad -\text{trace}\left(Z\right) \\ \text{trace}\left(\mathcal{H}_n Z\right) \leq 1 \quad n = 1 \ldots N \\ Z \succeq 0 \end{array} \tag{24}$$

This formulation allows us to solve optimization problem with usual SDP solvers, *i.e.*, SeDuMi [35]. Appendix B explains how to find energy distribution from the solution of optimization problem stated in Equation 24.

We have solved the above optimization problem for a network with 61 nodes, $E_s = 1mJ$, $E_r = 1mJ$, $E_f = 2mJ$, $\lambda' = 0.3\mu J^2$, and $\beta = 0.5$ (see Appendix B for β). Figure 6 shows the energy distribution for this asynchronous network.

C. BalancED-Base-s

Consider the scenario where there is a base-station v_b in the center of the hexagon; like the network shown in Figure 1. The node v_b is either the initial sender or the final reciever of the packets routed in the network. $R_{b,i}$ and $L_{b,i}$ denote the divisions of the space around v_b into lines and regions as described in Section V-A. The probability of being the initial sender or the final receiver for an arbitrary node v_n is again $\frac{1}{N}$. The forwarding energy is not the same as Balanced-P2P and is derived in Appendix C.

D. BalancED-Base-a

In the BalancED-Base-a case, all the formulation for the BalancED-P2P network remain valid except for the $p_{v_n \to v_m}$ terms in Equation 13. Recall $p_{v_n \to v_m}$ is the probability that node v_n sends a packet to the node v_m where v_n and v_m are two neighbor nodes. Therefore, we need to only find $p_{v_n \to v_m}$ for the new scenario.

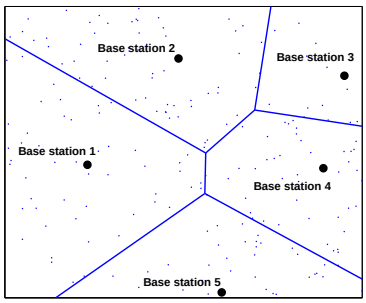

Fig. 7. Large sensor network with multiple base stations

Recall that all packets are routed on the shortest path to the base. Therefore, packets always go towards the center. Using the same notations that is used in Section BalancED-P2P-a, if v_n is on $L_{b,i}$, then $p_{v_n \to v_m}$ will be zero for all $v_m \in \mathcal{N}(v_n)$ except for $v_m \in \mathcal{N}(v_n) \cap L_{b,i}$ that will be $p_f(v_n) + \frac{1}{N}$. Note that $\frac{1}{N}$ is added to cover the case that v_n is the first sender. When v_n is in $R_{b,i}$, $p_{v_n \to v_m}$ will be zero for all $v_m \in \mathcal{N}(v_n)$ except for $v_i \in \mathcal{N}(v_n) \cap \left(L_{n,i+3(\text{mod } 6)} \cup L_{n,i+3(\text{mod } 6)}\right)$ that will be $\frac{1}{2}\left(p_f(v_n) + \frac{1}{N}\right)$.

Now that we have $p_{v_n \to v_m}$ for this scenario, we can plug it in Equation 13 to find the optimal energy distribution.

E. Extensions

In this section, we explain how we can extend the derived node distributions to randomly deployed networks and large networks with multiple base stations.

1) Randomly deployed networks: In the previous section, we assumed that all nodes are regularly located in an hexagonal area and we found energy distributions in the different scenarios. Here, we extend these distributions to the networks in which nodes are randomly deployed. All nodes have the same energy resource.

To increase the lifetime, nodes are distributed according to the derived energy distributions. For example, assume BalancED-P2P-a scenario. Nodes with the communication range r are deployed in an hexagonal area with diagonal d. We put $s = \lfloor \frac{d}{r} \rfloor$ and find BalancED-P2P-a energy distribution for an hexagonal with s nodes in the diameter. Next, the derived energy distribution is interpolated over the whole hexagonal area and is normalized to 1. This normalized distribution is used as the probability distribution function of the nodes in the area.

2) WANs with multiple base stations: Assume a network with hundreds of nodes and a number of base stations, as shown in Figure 7. Each node sends its data to the nearest base station, *i.e.*, Voronoi diagram of the base stations is constructed and each sensor sends its data to the base station in its Voronoi cell.

To have the optimal energy distribution in each Voronoi cell, one needs to find the optimal node distribution in all Voronoi cells. Generally, Voronoi cells are not symmetric structures, and thus the appropriate distribution cannot be easily and practically derived. Instead, we use the derived distribution for the regular hexagon as the energy distribution for these non-regular polygons. Using this method, we can extend the derived distributions to large networks with multiple base stations.

VI. Evaluation Results

We carried out extensive simulations to asses the performance of the BalancED distributions. First, for both fixed and randomly deployed networks, we compare BalancED-P2P and BalancED-Base networks. Second, synchronous and asynchronous networks are compared. Next, we study extending derived distributions to large networks with multiple base stations. Finally, sleep duration and packet delays are discussed.

The simulation set-up closely follows our assumptions in Section III. We define the size of the hexagonal area as the number of nodes that are on the diagonal of the hexagon. Thus, the size of the area in Figure 2 would be 7. In all of our deterministic evaluations, the size of the area, unless otherwise stated, is 7. In all simulations, we have used the energy consumption model derived in [28]. The model is based on LUCENT IEEE 802.11 Wavelan PC card. According to this model, if the length of each packet is 1Kb, each node consumes 2.35mJ to transmit and 0.856mJ to receive a packet. The model also suggests that the idle power consumption of nodes is 843mW. Thus, if we set λ of our sleeping protocol to $2.5mJ \times second$, λ' in Equation 14 will be $0.53\mu J^2$.

For the asynchronous scenarios, average sleep duration of each nodes is found by $\alpha_m = \frac{\lambda}{E_{step}(v_m)}$ (see Section V-B.) Where $E_{step}(v_m)$ is energy consumption of the node for each time step. Based on Appendix D, node v_m's sleep duration is an exponential random variable with mean equal to α_m.

To measure the network's lifetime, we run the network time step by step. In each time step, one node sends a packet to another node. The packet may be forwarded multiple times in each time steps. Nodes lose energy for sending a packet, forwarding a packet, receiving a packet, or staying in the idle mode. The first node that dies determines the network's lifetime.

In our evaluations, *fixed deployment* indicates the scenarios where nodes are regularly placed in the hexagonal area. Different nodes might have different amount of energies. In *random deployment*, all nodes have the same energy. In this case, nodes are distributed according to the derived distributions.

A. Comparing BalancED-P2P and BalancED-Base networks.

Equations 1 and 37 determine the expected required energy for each node for BalancED-P2P-s and BalancED-Base-s networks in hexagonal deployment. The expected energy is based on the probabilistic analysis for a single step. In real scenarios, if the total amount of available energy is not very large, the average usage of one node does not reach the asymptotic expectation, and thus, the network does not reach its full life-time efficiency. Asymptotically, for the network to last up to K steps, the initial energy of a node v_n should be at least $KE_{step}(v_n)$. We have varied the value of K, and observed the actual simulated lifetime of the network to study

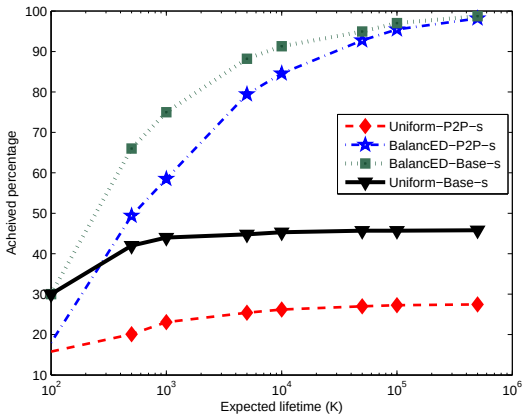

Fig. 8. Lifetime comparison for synchronous uniform and BalancED distributions.

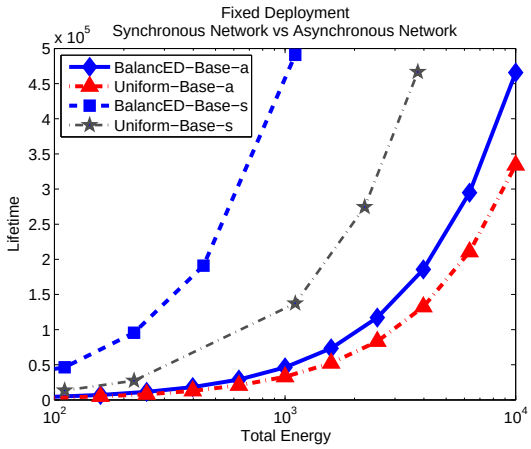

Fig. 10. Lifetime comparison for BalancED-Base-s, BalancED-Base-a, and uniform.

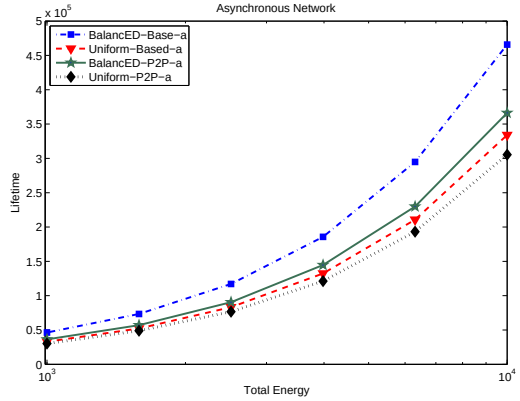

Fig. 9. Lifetime comparison for asynchronous uniform and BalancED distributions.

for which values of K the network reaches its asymptotic behavior. As we mentioned before, we consider a network dead when the first node dies.

Figure 8 shows the results. The horizontal axis is the expected lifetime (K) and the vertical axis is the achieved percentage of the expected lifetime. If the network's lifetime is K_s, then the vertical axis is $100\frac{K_s}{K}$. As it can be seen on the figure, BalancED networks can achieve 100% of their expected lifetime in high energy networks (more than 10^6 time steps). Also, BalancED-Base-s is more efficient than BalancED-P2P-s since it can achieve a higher lifetime efficiency with a lower energy.

In the next evaluation, we examine the efficiency of balanced distributions for asynchronous networks and random deployment. Figure 9 shows the results. The horizontal axis is the total energy of a network with 148 nodes. The vertical axis is network's lifetime in terms of number of steps. This figure indicates that balanced distributions perform about 20% better than uniform distributions for a random deployment.

B. Comparing synchronous and asynchronous communication.

Figure 10 compares BalancED-Base-s, BalancED-Base-a, and uniform distributions for fixed deployment. The horizontal axis is the total initial energy of the network and the vertical axis represents the network's lifetime. We run the simulation until the first nodes dies. The figure confirms that in the high-energy networks, synchronous paradigms are much more energy efficient compared with the asynchronous ones, because of the idle energy consumptions. We also observe that the BalancED-Base-s is three times more energy efficient than the uniform and the BalancED-Base-a is fifty percent more energy efficient than the synchronous uniform distribution.

Furthermore, cross section of the BalancED distributions are plotted in Figure 11. The observed discontinuity in the center of the Base-a and Base-s networks is because of the assumption of having the base-station with unconstrained amount of energy. In asynchronous networks, further nodes consume more idle energy than the nodes close to the center. Thus, the energy in asynchronous networks is more spread than in synchronous networks. Also, the figure confirms that the energy is more concentrated in the center in BalancED-Base when compared to the BalancED-P2P.

C. Number of alive nodes in time

We have also used NS-2 to monitor the number of alive nodes versus time. In this simulation, the wireless model in NS-2.30 is used. UDP, IEEE 802.11, and AODV [36] are used for network layer, MAC layer, and routing protocol, respectively. In this scenario, 100 nodes are randomly distributed in a hexagonal area (random deployment).

Two cases are considered for node distribution: BalancED-P2P-a and uniform. Diameter of the hexagonal area is 750m and the radio range of all nodes is 100m. Each node has 100mJ initial energy and simulation is run for 1500 steps. At the beginning of each step, two nodes, randomly, based on their locations, start to communicate, *i.e.*, one node sends a packet with length 500Kb to the other node. Figure 12 shows the result of this simulation. In the balanced distribution, most of

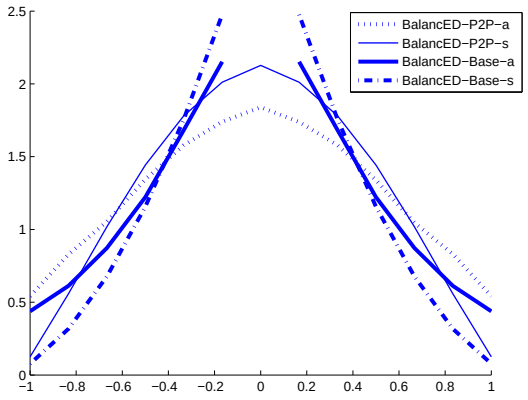

Fig. 11. Cross section of the derived distributions.

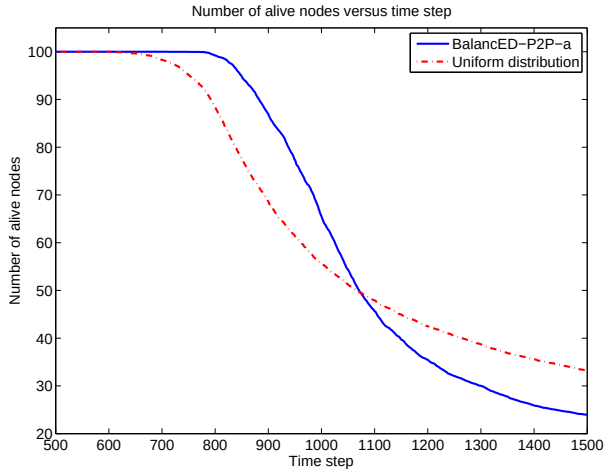

Fig. 12. Lifetime comparison for uniform and proposed distribution

the nodes live longer than the uniform distribution. The total initial energy in balanced and uniform networks is equal. As nodes start to die down, nodes in balanced distribution die faster than uniform distribution, *i.e.*, in balanced distribution, nodes' energies deplete almost at the same time.

D. Increasing the diagonal of monitoring area

In the next experiment, we examine the lifetime and the coverage. Table II shows networks' lifetime for different coverage areas (diagonal length of the area). The networks have the same amount of initial energies. Again, the BalancED-Base-s performs better than the BalancED-P2P-s. For instance, lifetime of a BalancED-Base-a with the diagonal of 20 is approximately the same as Balance-P2P-s lifetime with the diagonal 6. As expected, the networks' lifetime decreases linearly with the diagonal of the area.

In the next experiment, for random deployments, the nodes are distributed based on the BalancED-P2P-a distribution described in Section V. Table III illustrates the percentage of lifetime increase for the uniform and BalancED energy distributions for a random deployment. Networks with the same coverage area but different number of available energies

TABLE II
LIFETIME FOR DIFFERENT COVERAGE AREAS. THE TOTAL ENERGY OF THE NETWORK IS 10KJ.

Diagonal of area	BalancED-Base-s	BalancED-P2P-s
7	1.88×10^5	1.22×10^5
9	1.34×10^5	9.06×10^4
11	1.04×10^5	7.17×10^4
13	8.54×10^4	5.93×10^4
15	7.22×10^4	5.05×10^4
17	6.25×10^4	4.40×10^4
19	5.51×10^4	3.90×10^4
21	4.93×10^4	3.50×10^4

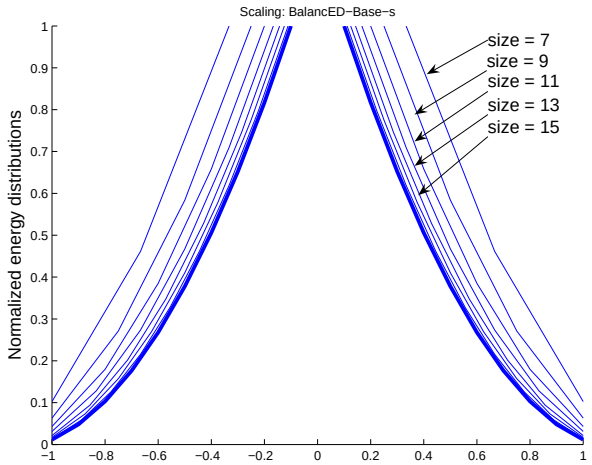

Fig. 13. Cross section of BalancED-Base-s distribution

are simulated. The first column is the number of nodes in the area. The second and third columns illustrate the percentage of lifetime increase for both synchronous and asynchronous cases respectively. By increasing the number of nodes, we gain more lifetime improvements. For BalancED-P2P-a, improvement over the uniform distribution increases from 22.07% for 200 nodes to 39.24% for 500 nodes in the network. The same behavior can be seen in BalancED-P2P-a networks. This is because as we increase the number of nodes, we get a better approximation of the continuous energy allocation.

TABLE III
EFFECT OF INCREASING THE NUMBER OF NODES

Number of nodes	Life increase (%) BalancED-P2P-s	Life increase (%) BalancED-P2P-a
200	22.07	44.66
300	22.69	46.94
400	26.60	43.44
500	39.24	53.66

Figure 13 shows the cross section of the BalancED-Base-s distributions by increasing the size of the monitoring area from 7 to 21. To have a comparable distributions, all plots are normalized. The figure suggests that, by increasing the diagonal of the area, energy distribution converges to the thick curve. The distance between eighth curve and the thick cure is less than 0.05 (L_1 distance of two curves).

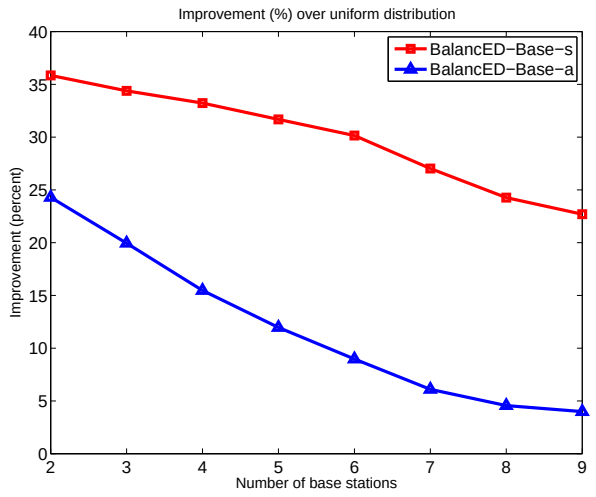

Fig. 14. Improvement (%) over uniform distribution versus number of the base stations

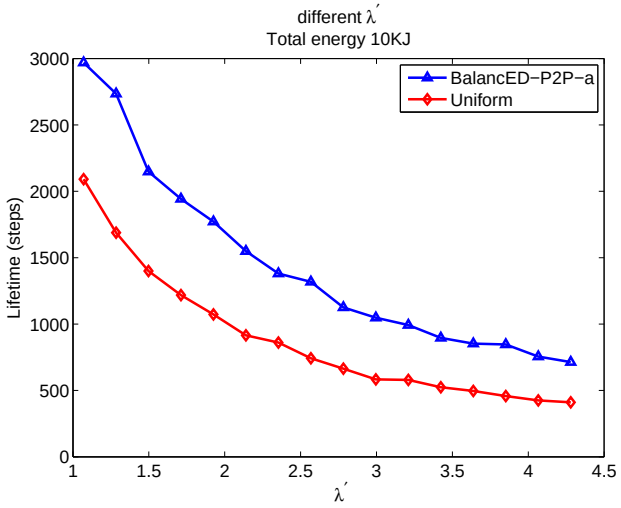

Fig. 15. Effect of sleep duration

E. Multiple base stations

We illustrate that the derived energy distributions can extend to distributed scenarios with multiple base stations. In this evaluation, 5000 nodes are randomly deployed. Location of the base stations is also randomly selected. As discussed in Section V-E2, in each Voronoi cell, BalancED-Base-s and BalancED-Base-a distributions are used. In networks with a small number of base stations, we obtain 25% and 35% improvements over the uniform distribution for asynchronous and synchronous networks. The improvement values decrease to 4% and 23% for networks with 9 base stations, respectively. Figure 14 shows the achieved improvement for both synchronous and asynchronous networks. By increasing the number of base stations, Voronoi cell become smaller. For very small Voronoi cells, balanced and uniform distributions are approximately the same. Thus, by increasing the number of base stations, less improvement over the uniform distribution is expected.

F. Lifetime and sleep duration in asynchronous networks

Furthermore, we have studied the effect of sleep duration on the network's lifetime. Since $\alpha_m = \frac{\lambda}{E_{totalstep}(m)}$, sleep duration of nodes is proportional to λ (thus with λ'). We have run simulation for different λ' and measured network lifetime for a fixed deployment. Figure 15 shows the lifetime versus λ'. In this simulation, the total energy of the network is 10KJ and nodes are randomly deployed. Figure 15 shows as the sleeping duration increases, the effect of non-uniform distribution increases, *i.e.*, as λ' increases from 1 to 4.3, improvement over uniform distribution increases from 42% to 75%.

G. Delay comparison

We also compare the packet delays for the balanced distributions versus the uniform distribution. The average delay of a synchronous network is proportional to the expected number of traversed hops. In asynchronous networks, the delay is also a function of the expected idle time. We have done extensive experiments measuring the delay of the asynchronous networks. Tables IV and V represent the results. In both P2P-a and Base-a networks of diagonal 7, we run the networks for a long time and averaged the encountered delays of the routes with the same number of hops. In both P2P-a and Base-a, the communications with less than 3 number of hops have less delays for the uniform distribution. However, the BalancED distributions have less delays for larger hop distances. For example, for a 5-hop distance, uniform distribution has a delay of 37.59 compared to 27.03 for the BalancED for the Base-a cases. Also uniform has a delay of 239 compared to 232 for the P2P-a cases. Note that in BalancED-Base networks, nodes only send packets to the base stations. Thus, the delays for these scenarios are smaller than the P2P scenarios.

TABLE IV
DELAY COMPARISON

# of hops	Uniform		Non-uniform	
	Delay (ms)	Percent	Delay (ms)	Percent
1	73.19	9.77	73.19	9.79
2	107.40	17.90	105.81	18.45
3	150.20	22.29	144.90	23.43
4	194.36	21.55	188.03	22.22
5	239.65	16.65	232.20	16.47
6	283.45	9.13	273.97	7.753
7	318.62	2.466	314.33	1.755
8	346.56	0.2045	338.47	0.1138
9	363.45	0.0029	453.78	0.0004
Avg delay(ms)	176.172		167.833	

VII. CONCLUSIONS

We have calculated the energy-balancing distribution of energies for ad-hoc wireless networks for the purpose of increasing the network's lifetime. We considered the peer-to-peer and base-station centric network architectures. Both synchronous and asynchronous communication paradigms were studied. For synchronous networks, we found the exact analytical solutions

TABLE V
DELAY COMPARISON

# of hops	Uniform-Base-a		BalancED-Base-a	
	Delay (ms)	Percent	Delay (ms)	Percent
1	0	10.92	0	11.19
2	9.6637	19.99	10.17	23.38
3	19.9445	38.45	20.08	43.90
4	27.4516	27.13	24.92	20.72
5	37.5902	3.49	27.03	0.78
Avg delay(ms)	18.36		16.57	

for the energy distribution in the network for a symmetric deterministic deployment. Next, we showed that finding the exact energy distribution for asynchronous networks is an NP-complete problem (rank one constraint). Thus, a convex formulation for the problem was used to approximate the optimal energy distribution. The derived distributions consider the effect of the idle energy consumption. Furthermore, we have extended the results to random networks and to distributed networks with multiple base stations.

We presented comparisons of the energy efficiency, coverage area, and delay encountered by the derived distributions and also the uniform distribution. We have also applied the derived energy distributions to randomly deployed networks and presented their energy efficiency. The evaluations show that, networks' lifetime of BalancED-Base scenarios are typically 20%-40% more than BalancED-P2P scenarios. Furthermore, we have shown that derived distributions do not increase the packet delays in the networks.

REFERENCES

[1] I. Stojmenovic and X. Lin, "Power-aware localized routing in wireless networks," *IEEE Transaction Parallel Distributed Systems*, vol. 12, no. 11, pp. 1122–1133, 2001.

[2] Y. Cui, Y. Xue, and K. Nahrstedt, "Pa utility-based distributed maximum lifetime routing algorithm forwireless networks," *IEEE Transaction Vehicular Technology*, vol. 55, no. 3, pp. 797–805, 2006.

[3] B. Yang, C. Long, X. Guan, and G. Feng, "Maximum lifetime rate control and scheduling in multi-hop wireless networks," in *IEEE International Conference on Networking, Sensing and Control*, 2006, pp. 619– 624.

[4] B. Bollobas, *Random Graphs*, 2nd ed. 40 West 20th Street, New York, NY 10011-4211, USA: Combridge University Press, 2001.

[5] M. Bhardwaj and A. Chandrakasan, "Bounding the lifetime of sensor networks via optimal role assignments," in *INFOCOM*, pp. 1587– 1596.

[6] B. Liu, Z. Liu, and D. Towsley, "On the capacity of hybrid wireless networks," in *INFOCOM*, 2003, pp. 1543–1552.

[7] A. Giridhar and P. R. Kumar, "Maximizing the functional lifetime of sensor networks," in *IPSN*, 2005, pp. 5–12.

[8] I. Paschalidis, L. Wei, and D. Starobinski, "Asymptotically optimal transmission policies for large-scale low-power wireless sensor networks," *IEEE/ACM Transactions on Networking (TON)*, pp. 105 – 118, Feb 2007.

[9] J. Hsu, S. Zahedi, A. Kansal, M. Srivastava, and V. Raghunathan, "Adaptive duty cycling for energy harvesting systems," in *ISLPED*, 2006, pp. 180–185.

[10] A. Iranli, M. Maleki, and M. Perdram, "Energy efficiency strategies for deployment of a two-level wireless sensor network," in *ISLPED*, 2006, pp. 2–10.

[11] G. Wang, M. Irwin, P. Berman, H. Fu, and T. Porta, "Optimizing sensor movement planning for energy efficiency," in *ISLPED*, 2005, pp. 215–220.

[12] O. Akan and I. Akyildiz, "Event-to-sink reliable transport in wireless sensor networks," *EEE/ACM Transactions on Networking (TON)*, vol. 13, no. 5, pp. 1003–1016, 2005.

[13] P. Taejoon and K. Shin, "Optimal tradeoffs for location-based routing in large-scale ad hoc networks," *EEE/ACM Transactions on Networking (TON)*, vol. 13, no. 2, pp. 398–410, 2005.

[14] C. Intanagonwiwat, R. Govindan, D. Estrin, J. Heidemann, and F. Silva, "Directed diffusion for wireless sensor networking," *IEEE/ACM Transactions on Networking (TON)*, vol. 11, no. 1, pp. 2–16, 2003.

[15] E. Uysal-Biyikoglu, B. Prabhakar, and A. E. Gamal, "Energy-efficient packet transmission over a wireless link," *EEE/ACM Transactions on Networking (TON)*, vol. 10, no. 4, pp. 487–500, 2002.

[16] M. Bhardwaj, A. Chandrakasan, and T. Garnett, "Upper bounds on the lifetime of sensor networks," in *ICC*, 2001, pp. 785 – 790.

[17] D. Ganesan, R. Cristescu, and B. Beferull-Lozano, "Power-efficient sensor placement and transmission structure for data gathering under distortion constraints," in *IPSN*, 2004, pp. 142–150.

[18] M. Maleki and M. Pedram, "Qom and lifetime-constrained random deployment of sensor networks for minimum energy consumption," in *IPSN*, 2005, pp. 293–300.

[19] A. Krause, C. Guestrin, A. Gupta, and J. M. Kleinberg, "Near-optimal sensor placements: maximizing information while minimizing communication cost," in *IPSN*, 2006, pp. 2–10.

[20] J. H. Chang and L. Tassiulas, "Maximum lifetime routing in wireless sensor networks," *IEEE/ACM Transactions on Networking (TON)*, pp. 609 – 619, August 2004.

[21] L. Hai, J. Xiaohua, W. Peng-Jun, Y. Chih-Wei, S. Makki, and N. Pissinou, "Maximizing lifetime of sensor surveillance systems," in *Networking, IEEE/ACM Transactions on*, April 2007, pp. 334–345.

[22] S. J. Baek and G. de Veciana, "Spatial energy balancing through proactive multipath routing in wireless multihop networks," *EEE/ACM Transactions on Networking (TON)*, vol. 15, no. 1, pp. 93–104, 2007.

[23] K. Kar, A. Krishnamurthy, and N. Jaggi, "Dynamic node activation in networks of rechargeable sensors," *EEE/ACM Transactions on Networking (TON)*, vol. 14, no. 1, pp. 15–26, 2006.

[24] P. Cheng, C. Chuah, and X. Liu, "Energy-aware node placement in wireless sensor networks," in *GLOBECOM*, vol. 5, 2004, pp. 3210–3214.

[25] Y. Chen, C. Chuah, and Q. Zhao, "Sensor placement for maximizing lifetime per unit cost in wireless sensor networks," in *MILCOM*, vol. 2, 2005, pp. 1097– 1102.

[26] R. Subramanian and F. Fekri, "Sleep scheduling and lifetime maximization in sensor networks: fundamental limits and optimal solutions," in *IPSN*, 2006, pp. 218–225.

[27] F. Koushanfar, N. Taft, and M. Potkonjak, "Sleeping coordination for comprehensive sensing using isotonic regression and domatic partitions," in *INFOCOM*, pp. 1– 13.

[28] L. Feeney and M. Nilsson, "Investigating the energy consumption of a wireless interface in an ad hoc networking environment," *INFOCOM*, vol. 3, pp. 1548–1557, 2001.

[29] www.xbow.com, "Mica2 mote datasheet," July,2003.

[30] C. B. Margi, K. Obraczka, and R. Manduchi, "Energy consumption trade-offs in sensor networks," in *presented at 2005 CITRIS Corporate Sponsor Day, on April 18th, 2005*.

[31] H. Zhang and J. C. Hou, "Maintaining sensing coverage and connectivity in large sensor networks," *Wireless Ad Hoc and Sensor Networks: An International Journal*, vol. 1, no. 1-2, pp. 89–123, 2005.

[32] R. Zheng, J. C. Hou, and L. Sha, "Asynchronous wakeup for ad hoc networks," in *international symposium on Mobile ad hoc networking computing*, 2003, pp. 35–45.

[33] M. Cardei and D.-Z. Du, "Improving wireless sensor network lifetime through power aware organization," *ACM Wireless Networks*, vol. 11, no. 3, pp. 333–340, 2005.

[34] F. Alizadeh, "Interior point methods in semidefinite programming with applications to combinatorial optimization," *SIAM Journal on Optimization*, vol. 5, no. 1, pp. 13–51, 1995.

[35] SeDuMi: self-dual minimization, "http://sedumi.mcmaster.ca/, seen in June, 2008."

[36] C. E. Perkins and E. M. Royer, "Ad hoc on-demand distance vector routing," in *Proceedings of the 2nd IEEE Workshop on Mobile Computing Systems and Applications*, 1999, pp. 90–100.

APPENDIX A
PROOF (ASYNCHRONOUS)

As was shown in Figure 5, we look for the probability that node v_n sends a packet to node v_m in one time step. Since the hexagonal area is symmetric, we only find $p_{v_n \to v_m}$ for the horizontal edges in the Figure 5. By using the same notations

introduced in the BalancED-P2P-s section, $p_{v_n \to v_m}$ can be found as follows.

$$\begin{aligned} p_{v_n \to v_m} &= \sum_{t \in \{0,5\}} p\left(v_n \to v_m \mid \mathcal{R}_{(v_n \to v_m)_t}\right) p\left(\mathcal{R}_{(v_n \to v_m)_t}\right) \\ &+ \sum_{s \in \{0,5\}} p\left(v_n \to v_m \mid \mathcal{S}_{(v_n \to v_m)_s}\right) p\left(\mathcal{S}_{(v_n \to v_m)_s}\right) \\ &+ p\left(v_n \to v_m \mid \mathcal{T}_{v_n \to v_m}\right) p\left(\mathcal{T}_{v_n \to v_m}\right) \\ &+ p\left(v_n \to v_m \mid \mathcal{Q}_{v_n \to v_m}\right) p\left(\mathcal{Q}_{v_n \to v_m}\right) \end{aligned} \tag{25}$$

where $v_n \to v_m = \{v_n \text{ send a packet to } v_m\}$; $\mathcal{R}_{(v_n \to v_m)_0} = \{R_{n,0} \cup L_{n,1} \to R_{m,3} \cup L_{m,4}\}$; $\mathcal{R}_{(v_n \to v_m)_5} = \{R_{n,5} \cup L_{n,5} \to R_{m,2} \cup L_{m,2}\}$; $\mathcal{S}_{(v_n \to v_m)_0} = \{R_{n,0} \cup L_{n,1} \to L_{m,3} \cup \{v_m\}\}$; $\mathcal{S}_{(v_n \to v_m)_5} = \{R_{n,5} \cup L_{n,5} \to L_{m,3} \cup \{v_m\}\}$; $\mathcal{T}_{v_n \to v_m} = \{L_{n,0} \cup \{v_n\} \to L_{m,3} \cup \{v_m\}\}$; and $\mathcal{Q}_{n \to m} = \{ L_{n,0} \cup \{v_n\} \to L_{m,2} \cup R_{m,2} \cup L_{m,3} \cup R_{m,3} \cup L_{m,4}\}$.

We use a similar approach that was used to find $p_f(v_n)$ in section V-A. Using Equation 5, non-conditional terms in Equation 25 can be easily found.

$\mathcal{R}_{(v_n \to v_m)_0}$ and $\mathcal{R}_{(v_n \to v_m)_5}$ can be found by using the same procedure that was used in Section V-B. The only difference is that when a packet arrives to v_n, there will be fifty percent chance that goes to v_m; therefore,

$$p\left(v_n \to v_m \mid \mathcal{R}_{(v_n \to v_m)_0}\right) = \frac{1}{2} \frac{1}{\mid R_{n,0} \mid + \mid L_{n,1} \mid} \times \sum_{v_m \in R_{n,0} \cup L_{n,1}} \frac{\begin{pmatrix} S_{v_m \to v_n,0} + T_{v_m \to v_n,0} \\ S_{v_m \to v_n,0} \end{pmatrix}}{2^{S_{v_m \to v_n,0} + T_{v_m \to v_n,0}}} \tag{26}$$

$$p\left(v_n \to v_m \mid \mathcal{R}_{(v_n \to v_m)_5}\right) = \frac{1}{2} \frac{1}{\mid R_{n,5} \mid + \mid L_{n,5} \mid} \times \sum_{v_m \in R_{n,5} \cup L_{n,5}} \frac{\begin{pmatrix} S_{v_m \to v_n,5} + T_{v_m \to v_n,5} \\ S_{v_m \to v_n,5} \end{pmatrix}}{2^{S_{v_m \to v_n,5} + T_{v_m \to v_n,5}}} \tag{27}$$

where $S_{v_m \to v_n,i}$ and $T_{v_m \to v_n,i}$ are defined in Section V.

Furthermore, to find $p\left(v_n \to v_m \mid \mathcal{S}_{(v_n \to v_m)_s}\right)$, we use similar expression as the Equation 11. Thus

$$p\left(v_n \to v_m \mid \mathcal{R}_{(v_n \to v_m)_0}\right) = \frac{1}{2\left(\mid R_{n,0} \mid + \mid L_{n,1} \mid\right)} \times \sum_{v_h \in R_{n,0} \cup L_{n,1}} \sum_{k=S_{v_m \to v_n,0}}^{S_{v_h \to v_n,0} + T_{v_h \to v_n,0}} \frac{\begin{pmatrix} k-1 \\ S_{v_h \to v_n,0} \end{pmatrix}}{2^{k-1}} \tag{28}$$

$$p\left(v_n \to v_m \mid \mathcal{R}_{(n \to m)_5}\right) = \frac{1}{2\left(\mid R_{n_5} \mid + \mid L_{n_5} \mid\right)} \times \sum_{v_h \in R_{n_5} \cup L_{n_5}} \sum_{k=T_{h \to n,5}}^{S_{m \to n,5} + T_{h \to n,5}} \frac{\begin{pmatrix} k-1 \\ T_{v_h \to v_n,5} \end{pmatrix}}{2^{k-1}} \tag{29}$$

Finally, we should derive $p\left(v_n \to v_m \mid \mathcal{T}_{v_n \to v_m}\right)$ and $p\left(v_n \to v_m \mid \mathcal{Q}_{v_n \to v_m}\right)$. When a node in $L_{n,0} \cup \{v_n\}$ sends a packet to a node in $L_{m,3} \cup \{v_m\}$, always v_n and v_m are on the unique shortest path between the sender and the receiver. Therefore, v_n has to forward the packet to v_m.

$$p\left(v_n \to v_m \mid \mathcal{T}_{v_n \to v_m}\right) = 1 \tag{30}$$

When $\mathcal{Q}_{v_n \to v_m}$, similar to Equation 11, the packet that is sent by $L_{n,0} \cup \{v_n\}$ can deviate from the $L_{n,0} \cup \{v_m, v_n\}$ at each forwarding step. Therefore,

$$p\left(v_n \to v_m \mid \mathcal{Q}_{v_n \to v_m}\right) = \frac{1}{\mid L_{n,0} \cup \{v_n\} \mid} \sum_{v_m \in L_{n_0} \cup \{v_n\}} \left(\frac{1}{2}\right)^{T_{v_m \to v_n,0}+1} \tag{31}$$

By putting all terms together, now we can find $p_{v_n \to v_m}$.

Appendix B
Optimal distribution derivation for the convex optimization solution

We use two methods to retrieve energy approximation from solution of convex optimization problem, Z_{opt}, in Equation 23.

In the first method, we use matrix decomposition. Since we have removed the rank one constrain, optimal value of Equation 24, Z_{opt}, is not a rank-one matrix. Therefore, retrieving $\mathcal{U}$ from Z_{opt} is not straight forward. If we have a rank-one approximation for Z_{opt}, denoted by $\hat{Z}_{opt}$, all columns of Z_{opt} will be parallel. The first element of $\mathcal{U}$ is one. Therefore, each column of $\hat{Z}_{opt}$ can be scaled to find $\mathcal{U}$; then, finding energy approximation, $\hat{E}_n^1$, from $\mathcal{U}$ is straight forward by Equation 15.

To approximate $\mathcal{U}$, we do singular value decomposition (SVD). In this method, we find the SVD of Z_{opt}.

$$Z_{opt} = W \Sigma \, V^T \tag{32}$$

where, W and V are two unitary matrices and Σ is a diagonal matrix that is not necessary a rank-one matrix. Singular values of Z_{opt} are diagonal elements of diagonal matrix Σ and are decreasingly ordered. If Z_{opt} was rank-one matrix, Σ would have only one non-zero element on its diagonal. Thus, a rank one approximation of Z_{opt} can be found by $\hat{Z}_{opt} = W \hat{\Sigma} V^T$ where $\hat{\Sigma}$ is obtained by putting all the diagonal elements of Σ to zero except for the first element.

In the second scheme for approximating the energy distribution, we examine the structure of Z. By definition of Z, the first column of Z is $\mathcal{U}$. We can easily select the first column of $\hat{Z}_{opt}$, and then Equation 15 would lead to an approximation for energy, $\hat{E}_n^2$

Now, we have two approximations for BalancED-P2P-a energy distribution and we will use combination of them.

$$\hat{E}_n = (1 - \beta)\hat{E}_n^1 + \beta \hat{E}_n^2 \tag{33}$$

where β is a combining coefficient ($0 \leq \beta \leq 1$).

APPENDIX C
FORWARDING PROBABILITY FOR BALANCED-BASE

In BalancED-Base-s scenario, to find forwarding energy that node v_n needs, we consider two cases: first, node v_n is located in $R_{b,i}$; second, node v_n is located in $L_{b,i}$ (for $i = 0...5$). If node v_n is located in $R_{b,i}$.

$$\begin{aligned} p_f(v_n) &= p_f(v_n \mid R_{n,i} \rightarrow v_b)\, p(R_{n,i} \rightarrow v_b) \\ &+ p_f(v_n \mid L_{n,i} \rightarrow v_b)\, p(L_{n,i} \rightarrow v_b) \\ &+ p_f\left(v_n \mid L_{n,i+1(\text{mode 6})} \rightarrow v_b\right) \times \\ &\quad p\left(L_{n,i+1(\text{mode 6})} \rightarrow v_b\right) \end{aligned} \tag{34}$$

Note that in these equations $R_{n,i}$ and $L_{n,i}$ refer to region allocation by node v_n and they are not the same as $R_{b,i}$ and $L_{b,i}$. From Subsection V-A, it is clear that

$$\begin{aligned} &p(v_n \mid R_{n,i} \rightarrow v_b) = p\left(v_n \mid R_{n,i} \rightarrow R_{n,i+3(\text{mode 6})}\right) \\ &p(v_n \mid L_{n,i} \rightarrow v_b) = p(v_n \mid L_{n,i} \rightarrow G_{n,i}) \\ &p\left(v_n \mid L_{n,i+1(\text{mode 6})} \rightarrow v_b\right) = \\ &\qquad p\left(v_n \mid L_{n,i+1(\text{mode 6})} \rightarrow G_{n,i+1(\text{mode 6})}\right) \end{aligned} \tag{35}$$

All the expressions in the right hand of above equations were derived earlier; all elements of Equation 34 can be found from Equations 6, 12, and 5.

Now consider the case that v_n is in $L_{b,i}$. Again, we can write

$$\begin{aligned} p_f(v_n) &= \sum_{j=-1}^{0} p_f(v_n \mid \mathcal{V}_{i,j})\, p(\mathcal{V}_{i,j}) \\ &+ \sum_{j=-1}^{0} p_f(v_n \mid \mathcal{W}_{i,2j+1})\, p(\mathcal{W}_{i,j}) \\ &+ p_f(v_n \mid \mathcal{U}_i)\, p(\mathcal{U}_i) \end{aligned} \tag{36}$$

where $\mathcal{V}_{i,j} = \left\{R_{n,i+j(\text{mode 6})} \rightarrow v_b\right\}$, $\mathcal{W}_{i,j} = \left\{L_{n,i+j(\text{mode 6})} \rightarrow \{v_b\}\right\}$, and $\mathcal{U}_{i,j} = \{L_{n,i} \rightarrow \{v_b\}\}$. In these equations, we can also replace $L_{n,i+3(\text{mode 6})}$ instead of v_b and find their value from Equations 5, 10, and 11.

Now, we can find the total energy that each node requires at each time step as follows.

$$E_{step}(n) = \frac{1}{N} E_s + p_f(v_n)\, E_f \tag{37}$$

APPENDIX D
FINDING IDLE TIME

Figure 16 shows the working cycles of nodes in asynchronous scenarios. A node v_n wakes up periodically and checks for the packets. If there is a packet, the nodes receives it; otherwise, it sleeps for a random period of time. If node v_m wants to send a packet to v_n at time t, it should wait $\mathbf{h}$ seconds until node v_n wakes up (Figure 16.)

Assume the wake up time is a Poisson random process. Thus, sleep duration ($\mathbf{T}_s$) is a random variable which is exponentially distributed. i.e., if mean of sleep duration is α then

$$f_{\mathbf{T}_s}(T_s) = \frac{1}{\alpha} e^{\frac{T_s}{\alpha}}.$$

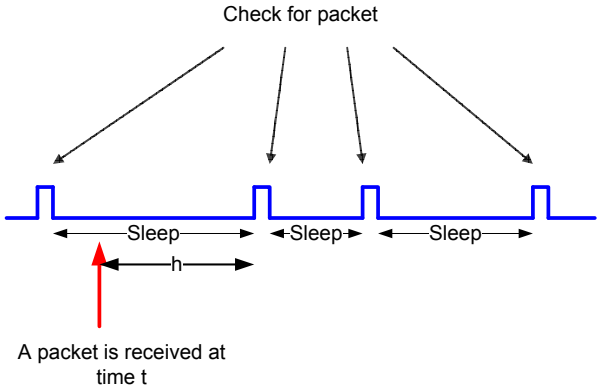

Fig. 16. In BalancED-p2p-a abd BalancED-base-a, nodes sleep random durations to save energy.

Since $\mathbf{T}_s$ is exponentially distributed, it is memoryless; i.e.,

$$f_{\mathbf{T}_s}(T_s | T_s > t) = \frac{1}{\alpha} e^{\frac{T_s - t}{\alpha}}.$$

Thus, waiting time $\mathbf{h}$ is also an exponential random variable and

$$E\{\mathbf{h}\} = \alpha.$$

Node v_m, in average, should wait α second for node v_n to wake up.

Davood Shamsi received his B.Sc. degree in electrical engineering and mathematics from Sharif University of Technology in 2006. Then, he joined Electrical and Computer Engineering school of Rice university for graduate study. He is currently working on sensitivity analysis in continuous and discrete optimization and optimal energy sensor networks.

Farinaz Koushanfar is an assistant professor at the departments of Electrical and Computer Engineering (ECE) and Computer Science (CS) at Rice University since July 2006. Her research interests are in distributed embedded systems, sensor-based embedded systems, data integrity, hardware security and intellectual property protection. She has finished her PhD in Electrical Engineering and Computer Science, and her MA in Statistics at UC Berkeley in December 2005. Prior to joining Rice, she held the Coordinated Science Lab (CSL) fellowship at the University of Illinois Urbana-Champaign. She is the recipient of the DARPA/MTO Young Faculty Award across all core technology areas, and the NSF CAREER Award. She has also received Intel Open Collaborative Research fellowship, a best paper

award at Mobicom, NSF graduate student fellowship, and the UCLA Woman4change leadership award.